

# Structure–Properties Relations of the Drawn Poly(ethylene terephthalate) Filament Sewing Thread

Andreja Rudolf, Majda Sfiligoj Smole

Department of Textiles, Faculty of Mechanical Engineering, University of Maribor, Smetanova 15, 2000 Maribor, Slovenia

Received 23 February 2006; accepted 23 June 2006

DOI 10.1002/app.25008

Published online 26 August 2008 in Wiley InterScience (www.interscience.wiley.com).

**ABSTRACT:** This article presents research into draw ratio influence on the structure–properties relationship of drawn PET filament threads. Structural modification influence due to the drawing conditions, i.e., the birefringence and filament crystallinity, on the mechanical properties was investigated, as well as the shrinkage and dynamic mechanical properties of the drawn threads. Increasing draw ratio causes a linear increase in the birefringence, degree of crystallinity, filament shrinkage, and a decrease in the loss modulus. In addition, loss tangent and glass transition tempera-

ture, determined at the loss modulus peak, were increased by drawing. The observed structural changes influence the thread's mechanical properties, i.e., the breaking tenacity, elasticity modulus, and tension at the yield point increase, while breaking extension decreases by a higher draw ratio. © 2008 Wiley Periodicals, Inc. *J Appl Polym Sci* 110: 2641–2648, 2008

**Key words:** PET sewing thread; drawing; birefringence; DSC; DMA; mechanical properties

## INTRODUCTION

Sewing thread has a geometry of parallel filaments that are twisted to achieve sufficient cohesiveness. Therefore, filaments are inclined under a defined twist angle in regard to the longitudinal thread axis. Filament threads for the automotive industry are usually produced from 100% polyamide (PA) or poly(ethylene terephthalate) (PET) multifilament, i.e., as plied thread, consisting of two or more yarns, containing numerous continuous filaments. Filament threads for the sewing of car seat covers have to fulfil high quality demands regarding strength, elasticity, and friction characteristics. In addition, high stitching speed and, thereby, technologically conditioned forces produce high thread loadings.

The behavior of a sewing thread during the sewing process directly influences the assurance of sewing process reliability, when it comes to the dynamic and thermal thread loadings. Thread load during the sewing process particularly influences the mechanical properties of the thread, which depend on filaments' inherent properties and on the complex arrangements of filaments in the thread's construction. Therefore, to assure appropriate properties, a sewing thread undergoes a drawing process at the elevated temperature, to improve the thread's mechanical properties, but above all to increase the breaking tenacity and elasticity

modulus, the tension at the yield point, and to decrease the coincident breaking extension.

Like most polymer materials, sewing threads also display viscoelastic properties, which are conditioned by filament's supramolecular structure, i.e., the crystallinity and orientation. In fibers, polymer molecules are organized in amorphous and crystalline regions, preferentially oriented along the fiber axis and linked by intra- and intermolecular bonds. The properties of a polymeric material can be enhanced significantly through the orientation processes. Mechanical and thermal effects influence macromolecular motions and, thus, change filaments' mechanical properties when drawing at elevated temperature, depending on the tensile force and thermal conditions.<sup>1,2</sup> In fact, many morphological modifications, such as conformational changes, strain-induced crystallization, and variation in crystal size and distribution, are involved when drawing and, thus, orienting PET.<sup>3,4</sup> For the production of high-quality thread with appropriate resistance against dynamic load during the sewing process, it is necessary to concentrate attention on the study of the tension at the yield point. Namely, the tensile force of the thread during sewing must not exceed the thread tension at the yield point, otherwise the first permanent deformations of the thread will arise.<sup>5</sup>

There has been a lot of research work on studying drawing and thermal treatment's influence on filament's properties,<sup>4,6–14</sup> but the exact relationship between the drawing conditions, structural changes, and mechanical properties of the drawn sewing thread's filaments, as yet have not been established.

Correspondence to: A. Rudolf (arudolf@uni-mb.si).

Therefore, the aim of the research was to find a structure–property relation of the drawn PET filament sewing thread.

## EXPERIMENTAL

### Materials and sample preparation

Commercial multifilament PET yarn of 28/72/0, i.e., yarn linear density 28 tex (1 tex = 1 g/1000 m), 72 filaments, zero twist, produced by SANS Fibers, was used for the production of a 3-ply and Z-twisted thread with 210 turns/m. After the dyeing process, the thread was drawn on an Edmund Erdman drawing machine, type DMW 08/190, and afterwards surface-treated with a lubrication agent.

A five-step drawing process was carried out on heated cylinders by using different draw ratios, namely  $\lambda_{1-5} = 1.05, 1.10, 1.15, 1.20,$  and  $1.25$ , while the constant drawing conditions were as follows:

Temperature of the first heated cylinder,  $T_1 = 120^\circ\text{C}$ ;

Number of turns that defines the contact time of the thread with the first heated cylinder,  $n_1 = 11$  turns;

Temperature of the second heated cylinder,  $T_2 = 200^\circ\text{C}$ ;

Number of turns that defines the contact time of the thread with the second heated cylinder,  $n_2 = 5$  turns;

Drawing speed,  $v = 400 \text{ m min}^{-1}$ ;

The drawn threads' samples are marked by  $C_1$  ( $\lambda_1 = 1.05$ ),  $C_2$  ( $\lambda_2 = 1.10$ ),  $C_3$  ( $\lambda_3 = 1.15$ ),  $C_4$  ( $\lambda_4 = 1.20$ ), and  $C_5$  ( $\lambda_5 = 1.25$ ), according to the draw ratio employed.

### Methods

Different analytical methods, such as calorimetric measurements, birefringence determination, dynamic mechanical, and tensile measurements, were used for evaluation of the structural parameters and determination of the drawn threads' mechanical properties, respectively. These methods are described in detail in Refs. 15–23. The properties of the undrawn yarn and drawn threads were evaluated, as well as the properties of the filaments from the yarn and threads. For this reason, the filaments were separated from the yarn and drawn thread samples.

A compensation method according to Ehringhaus was used for filament birefringence determination on an Ortholux Polarization microscope (Leitz–Wetzlar). The diameter of the filament was measured microscopically using an eye-piece micrometer. The filaments birefringence was observed at a wavelength of

546.1 nm (white light) and calculated [cf. eq. (1)] from these measurements.<sup>17</sup>

$$\Delta n_s = \frac{\Gamma_\lambda}{d} \quad (1)$$

where  $\Delta n_s$  is the birefringence of the sample;  $\Gamma_\lambda$  is the phase difference for used wavelength of the light (nm);  $d$  is the diameter of the filament ( $\mu\text{m}$ ).

The melting enthalpy was determined by differential scanning calorimetry (DSC) using the DSC-TA-4000-Mettler Toledo measuring system. Each thermogram was recorded from 25 to  $350^\circ\text{C}$ . The heating rate was  $10^\circ\text{C}/\text{min}$ . The melting enthalpy ( $\Delta H_{\text{ms}}$ ) was determined from the area of the curve's endothermic peak. The degree of crystallinity ( $\alpha_{\Delta H}$ ) was calculated from the determined melting enthalpy [cf. eq. (2)].<sup>20</sup> The melting enthalpy of the ideal crystalline PET of  $140.1 \text{ J/g}$  was used for calculation.<sup>21</sup>

$$\alpha_{\Delta H} = \frac{\Delta H_{\text{ms}}}{\Delta H_{\text{mc}}} \quad (2)$$

where  $\Delta H_{\text{ms}}$  is the melting enthalpy of the sample (J/g);  $\Delta H_{\text{mc}}$  is the melting enthalpy of the ideal crystalline PET (J/g).

Measurements of the filaments' dynamic mechanical properties were carried out using a Perkin–Elmer DMA7 measuring system at a constant frequency of 10 Hz. We started the experiment at a temperature of  $30^\circ\text{C}$ , with a static force 500 mN, dynamic force 400 mN, and we used a heating rate of  $5^\circ\text{C}/\text{min}$ . Samples were prepared in the form of a 72-filament bundle. The  $\beta$ -relaxation transitions (glass-transition) were determined with dynamic mechanical analysis, which are a consequence of movements of the molecular segments in the amorphous regions. The results were calculated and graphically processed by a program operating at the measuring system. The following are equations for calculation of the viscoelastic parameters [cf. eqs. (3) and (4)]:

$$E'' = \frac{\omega D}{k} E' \quad (3)$$

$$\tan \delta = \frac{E''}{E'} \quad (4)$$

where  $E''$  is the loss modulus, which corresponds to a viscosity representing the energy lost in the form of heat (Pa);  $\tan \delta$  is the loss tangent (loss factor);  $E'$  is the storage modulus, which corresponds to a spring constant representing the extent of energy stored in the sample (Pa);  $\omega$  is the frequency (rad/s);  $D$  is the sample damping factor (mN s/mm);  $k$  is the sample spring constant (mN/mm).

Loss tangent ( $\tan \delta$ ) and loss modulus ( $E''$ ) were determined at the relaxation transitions maxima, as well as the temperature of the loss modulus ( $T_{E''}$ ), which is used for interpretation of the glass transition

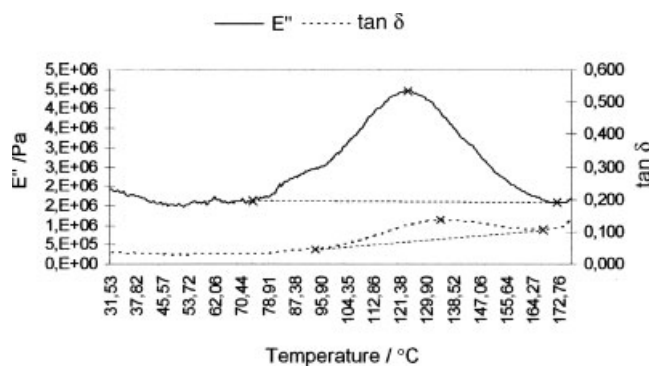


**Figure 1** Analysis of the relaxation transitions of the DMA curves.

temperature (Fig. 1). Filament loss modulus  $E''_{\max}$  represents molecular relaxation processes in the noncrystalline regions of the polymer, and it is a function of the amount and degree of orientation of the noncrystalline chains in the sample,<sup>14</sup> consequently, a higher amorphous orientation causes a lower loss modulus. Therefore, we used it as a criterion for the estimation of the amorphous orientation.

The shrinkage of the drawn threads in boiling water was determined according to the standard method ASTM D2102,<sup>15</sup> and calculated using the expression [cf. eq. (5)]:

$$S = \frac{(L_0 - L_s)}{L_0} \times 100 \quad (\%) \quad (5)$$

where  $L_0$  is the initial length of the thread and  $L_s$  is the thread's length after the treatment.

Thermally induced shrinkage occurs as a result of disorientation of the oriented noncrystalline regions of the fibers. Therefore, a higher orientation of the noncrystalline regions is a reason for higher fiber shrinkage.<sup>24</sup>

In addition, the mechanical properties of the filaments and threads were determined.

The measurements of the filaments' mechanical properties were carried out on a Vibrodyn 400 dynamometer, connected to a Vibroskop 400 linear density measuring device, according to the standard test method ISO 5079.<sup>19</sup> Breaking tenacity, breaking extension, and elasticity modulus at 1% extension were calculated from the obtained results. Measurements were carried out under standard conditions.<sup>22</sup>

Threads' mechanical properties were measured on an Instron 6022 dynamometer according to the standard test method ISO 2062.<sup>18</sup> The measurements were performed under standard conditions.<sup>22</sup> A mean stress-strain curve was constructed from the measurements and the viscoelastic parameters were calculated and determined from the mean curve,<sup>16</sup> and from the first, second, and third derivative of the experimental curves ( $\sigma'$ ,  $\sigma''$ ,  $\sigma'''$ ), respectively (Fig. 2). The elasticity modulus ( $E_0$ ) was determined at the gradation points of the first derivative curve, where the second derivative curve crosses the  $x$ -axis. The tension at the yield point ( $\sigma_y$ ) was determined on the curve  $\sigma(\varepsilon)$  at the position of  $\sigma'''(\varepsilon) = 0$ . The linear density of the threads was determined according to the standard test method ISO 1889.<sup>23</sup>

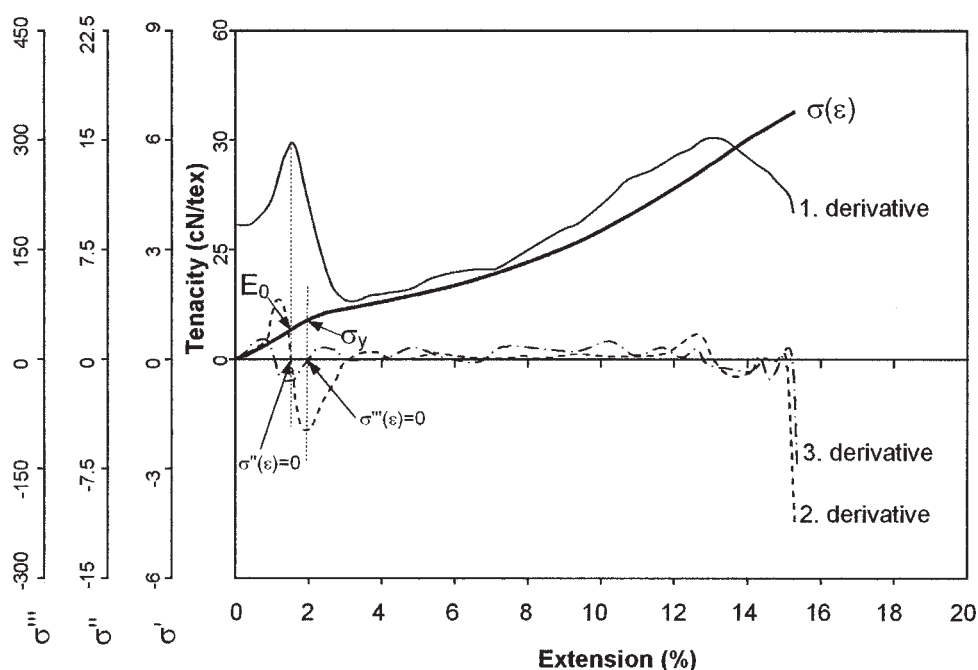


**Figure 2** Viscoelastic properties of the thread, determined from the stress-strain curve  $\sigma(\varepsilon)$ .

**TABLE I**  
Structural Parameters of the Undrawn Yarn's Filament and Drawn Threads' Filaments

Draw ratio, $\lambda$	Degree of crystallinity, $\alpha_{\Delta H}$	Birefringence, $\Delta n$	Loss tangent, $\tan \delta_{\max}$	Loss modulus, $E''_{\max}$ ( $10^6$ ) (Pa)	Temperature of loss modulus, $T_{E''_{\max}}$ ( $^{\circ}\text{C}$ )	Shrinkage, $S$ (%)
–	0.390	0.2127	0.131	4.48	124.21	1.32
1.05	0.438	0.2090	0.149	5.00	128.11	0.29
1.10	0.459	0.2142	0.139	4.28	129.41	0.81
1.15	0.456	0.2173	0.142	4.56	130.39	2.80
1.20	0.463	0.2183	0.157	3.87	129.08	2.42
1.25	0.457	0.2229	0.129	3.99	124.40	3.84

## RESULTS AND DISCUSSION

The structural parameters and properties of the undrawn and untwisted PET yarn's filaments are presented in Tables I and II, while the characteristics of the drawn threads and the filaments are presented in Figures 4 and 5.

The crystallinity degree, determined from the DSC curves (Fig. 3), of 0.390 was found for the untreated filament. The drawing conditions increase the degree of crystallinity, which achieves its highest value of 0.463 for the filament that was drawn at the draw ratio of 1.20 [Fig. 4(a)]. The birefringence is 0.2127 for the untreated filament. The drawing process increases molecular orientation, as confirmed by the measurements of the filament's birefringence. When the draw ratio of 1.25 is used,  $\Delta n$  is 0.2229 [Fig. 4(a)]. The  $\beta$ -relaxation transitions maxima (glass-transition) of the untreated filament are: loss tangent 0.131, loss modulus  $4.48 \times 10^6$  Pa, while the temperature at the loss modulus maximum is  $124.21^{\circ}\text{C}$ . With the increasing draw ratio, the loss tangent and temperature of the loss modulus maximum increase, while the loss modulus decreases [Figs. 4(b) and 4(c)]. The loss tangent has the maximal value when the draw ratio of 1.20

( $\tan \delta_{\max} = 0.157$ ) was used, while the loss modulus achieved the minimal value of  $3.87 \times 10^6$  Pa at the same draw ratio. The temperature of the loss modulus maximum, i.e., the glass transition temperature, achieves the highest value of  $130.39^{\circ}\text{C}$  for the filament that was drawn at the draw ratio of 1.15. Shrinkage of the undrawn filament has the value of 1.32%. After drawing, it achieves the highest value of 3.84% for the filament drawn at the highest draw ratio ( $\lambda_5 = 1.25$ ) (Fig. 4). However, the trend of a linear increase in the degree of crystallinity, birefringence, and shrinkage, as well as linear decrease in the loss modulus with increasing draw ratio was observed (Fig. 4). A decrease in the filament birefringence and shrinkage, as well as an increase in the loss modulus when compared the undrawn yarn and drawn thread at the draw ratio of 1.05 is attributed to the dyeing process of the thread in apparatus before drawing, which probably increases the crystallinity and molecular disorientation in the noncrystalline regions (Table I). With the increasing draw ratio, the decrease in the  $E''_{\max}$  is attributed to higher resistance on thermal movements of the macromolecular segments in noncrystalline regions by strain-induced increase of the amorphous orientation, which shows also the

**TABLE II**  
Mechanical Properties of the Undrawn Yarn, Drawn Threads, and Their Filaments

Sample type	Draw ratio, $\lambda$	Breaking tenacity, $\sigma_b$ ( $\text{cN tex}^{-1}$ )	Breaking extension, $\epsilon_b$ (%)	Elasticity modulus, $E_0$ ( $\text{cN tex}^{-1}$ )	Tension at yield point, $\sigma_y$ ( $\text{cN tex}^{-1}$ )
Yarn	–	62.09	13.54	7.60	11.62
Yarn's filaments	–	70.80	17.60	548	–
Drawn threads					
C <sub>1</sub>	1.05	56.60	19.85	4.70	8.30
C <sub>2</sub>	1.10	57.36	18.40	4.75	8.37
C <sub>3</sub>	1.15	57.75	15.89	5.80	8.28
C <sub>4</sub>	1.20	58.53	15.27	7.82	8.46
C <sub>5</sub>	1.25	61.81	14.38	6.25	9.27
Drawn threads' filaments					
C <sub>1</sub>	1.05	67.5	21.0	354	–
C <sub>2</sub>	1.10	69.7	18.2	389	–
C <sub>3</sub>	1.15	69.9	17.8	392	–
C <sub>4</sub>	1.20	71.3	16.4	411	–
C <sub>5</sub>	1.25	71.3	14.4	467	–



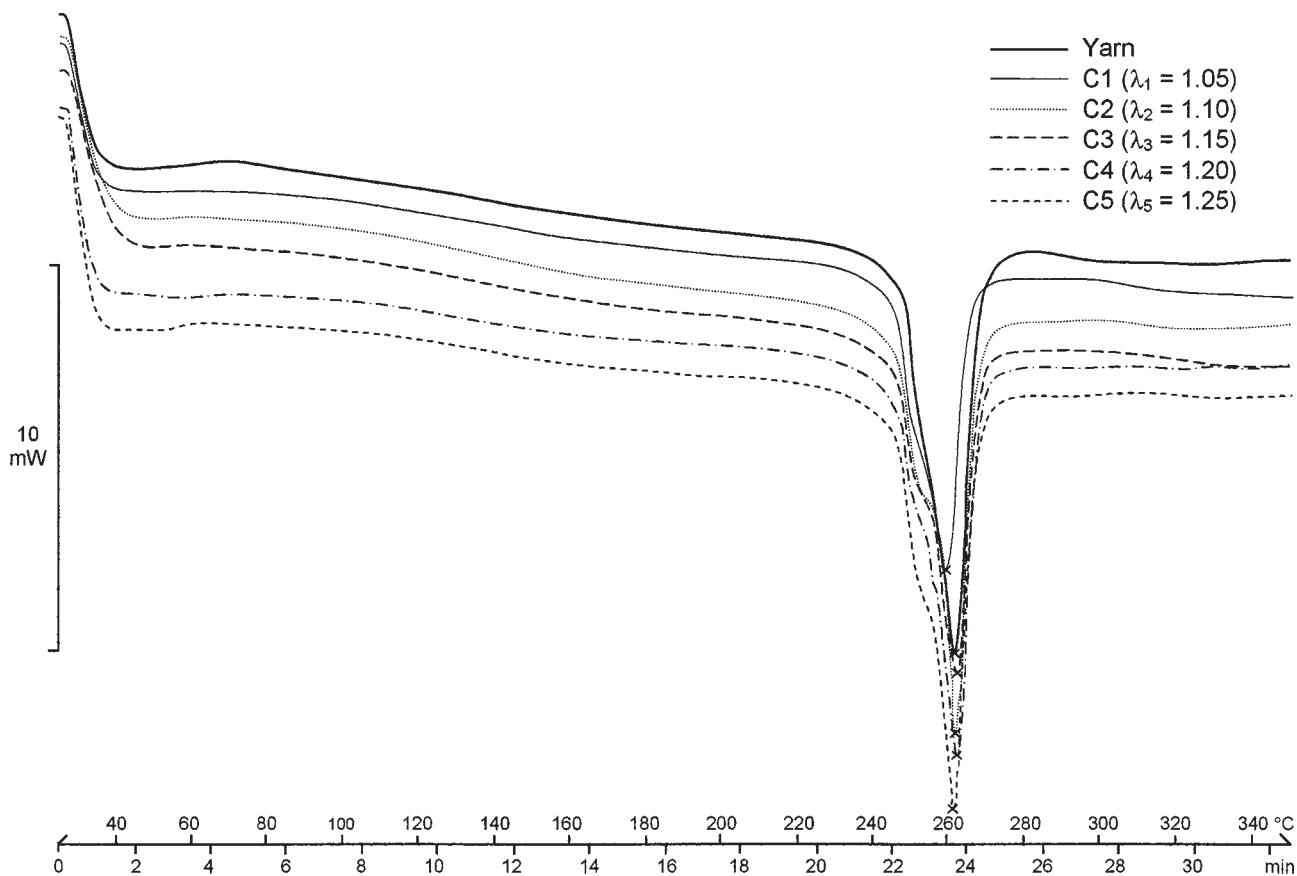
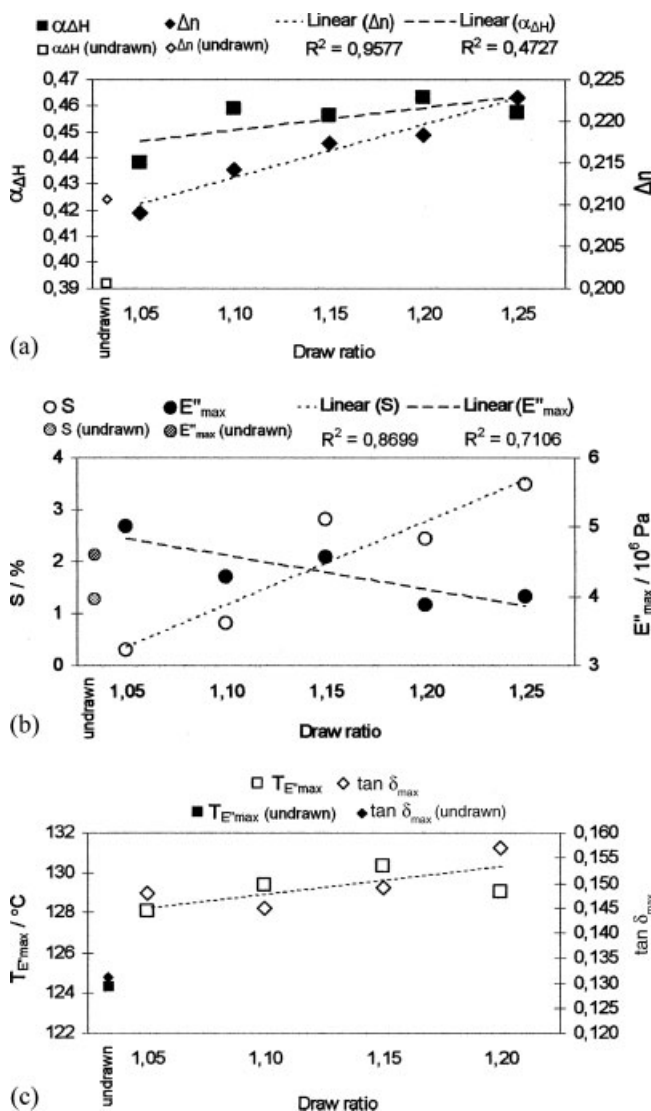


Figure 3 DSC thermograms of the undrawn and drawn samples.

increased shrinkage. With increasing draw ratio, the  $E''$  is changed from the sharp-high relaxation transition into the broad-low relaxation transition. By drawing induced increase in the amorphous orientation contributes also to increase in the glass transition temperature and the loss tangent. The results of our investigation confirm the results obtained by Murayama.<sup>1</sup> Namely, it was found that increasing the draw ratio increases the degree of crystallinity and the temperature of the loss modulus maximum  $T_{E''_{max}}$ ,  $T_g$  respectively, while the loss modulus decreases with the draw ratio.<sup>1</sup> When vibrating hot drawing on PET fiber is applied, it was found from temperature and intensity of relaxation transition (glass-transition) that the movements of amorphous chains are strongly inhibited.<sup>25</sup> With regard to the findings of Van den Heuvel et al.<sup>26</sup> and Aji et al.,<sup>3</sup> we suppose that drawing increases the trans conformation in the noncrystalline molecules, because macromolecules of the taut thread's filaments above the glass transition temperature ( $T_1 = 120^\circ\text{C}$ ) tend to arrange along the filament's axis when straightening. Therefore, the amount of gauche conformations diminishes and proceeds to trans conformations. By laser-heating zone-drawn of the PET spun fiber, Suzuki and Mochiduki<sup>27</sup> found by FTIR measurements that a trans conformation increased and a gauche one decreased. However, draw-

ing above the glass transition temperature increases the tensile deformation, which probably causes the straightening and sliding of the strained intrafibrillar tie molecules, which proceeds to the crystalline domains. This is confirmed by the higher degree of crystallinity, and the birefringence after the drawing process. In addition, the increased degree of crystallinity possibly arises from<sup>1</sup> the growth of the crystallites and<sup>2</sup> formation of new crystallites. Higher orientation also increases the glass transition temperature. The glass transition temperature, which is influenced by molecular orientation and loss tangent, increases when drawing to a draw ratio of 1.20 (Fig. 4). There are some structural changes observed that are unexpected, i.e., a decrease in the glass transition temperature and loss tangent is observed at the draw ratio of 1.25. They are attributed to very extend and unexpressive peaks of the  $\beta$ -relaxation transitions when the draw ratio of 1.25 was used. Because of the shape of the curves, it is not possible to precisely determine the peaks. The reason for extended relaxation transitions is increased degree of crystallinity, molecular orientation, and many other structural parameters by drawing, which have influence on shape and intensity of the relaxation transitions. On the other hand, the unexpected structural changes and deviations from the determined trend lines are attributed to the non-



**Figure 4** Structural parameters of the undrawn yarn and drawn threads' filaments: (a) degree of crystallinity/birefringence, (b) shrinkage/loss modulus, (c) temperature at the loss modulus maximum/loss tangent.

uniform treatment of the filaments due to their different position in the thread's cross sections. In addition, different treatment conditions, especially thermal conditions, influence the filament's properties. Namely, only a part of the threads' filaments are in direct contact with the heating cylinder. It should be stated that textile fibers are generally nonhomogeneous and, therefore, slight changes in structure sometimes reflect property variations along the fiber axis.

The maximum for the loss modulus of a PET fiber usually attains values of about  $10^9$  Pa.<sup>1</sup> Because of the special conditions at which the measurements of the drawn threads were performed, i.e., the dynamic mechanical properties were determined for the bundle of filaments, the maximum for the loss modulus has a magnitude of  $10^6$  Pa. Provided that  $E''_{max}$  is mathe-

matically calculated for a single filament, our results reach general values. On the other hand, it is possible that the thread twist influences the values of the loss modulus. This is confirmed by the study of the effect of geometric twist on dynamic modulus.<sup>1</sup> This study observed the reduction of the dynamic modulus by increasing yarn twist due to stress distribution in the thread, generated by the thread geometry.

Modification of the filaments' structure affects changes in the filaments' mechanical properties, which is also reflected in the changes of the threads' mechanical properties. The mechanical properties of the untreated yarn's filament are: breaking tenacity 70.80 cN/tex, breaking extension 17.6%, and elasticity modulus 548 cN/tex, while mechanical properties for the untreated yarn are:  $\sigma_b = 62.09$  cN/tex,  $\varepsilon_b = 13.54\%$ ,  $E_0 = 7.60$  cN/tex, and  $\sigma_y = 11.62$  cN/tex. After drawing, the mechanical properties of the filaments and threads were changed (Fig. 5). The drawing process at a higher draw ratio forms a more satisfactory fibrillar structure and, thereby, an increase in the breaking tenacity, elasticity modulus, and tension at the yield point is observed, while breaking extension linearly decreases with increasing draw ratio. We can conclude that a higher draw ratio improves the tensile properties of the drawn samples. The breaking tenacity of the filament achieves the highest value of 71.30 cN/tex at the draw ratio of  $\lambda_5 = 1.25$ , while the breaking tenacity of the thread has the highest value of 61.81 cN/tex at the highest draw ratio. When the draw ratio of 1.25 is used, the breaking extension of the filament is 14.40% and for the thread it is 14.38%, and the elasticity modulus of the filament is 467 cN/tex and for the thread it is 7.82 cN/tex, respectively. The tension at the yield point, which was determined only for threads, achieves the highest value at the draw ratio of 1.25 ( $\sigma_y = 9.27$  cN/tex). Deviation from the linear trend shows the elasticity modulus for the thread of type C4 ( $\lambda_4 = 1.20$ ) and tension at the yield point for the thread of type C3 ( $\lambda_3 = 1.15$ ). Our results coincide with the observations of different researchers who established that increasing draw ratio increases the crystallinity, birefringence, and amorphous orientation of the drawn yarn's fibers/filaments,<sup>4,7,8,13,14,28</sup> which is the reason for an increase in the elasticity modulus, breaking tenacity, and a decrease in the breaking extension. However, the mechanical properties of the threads' filaments in comparison to the untreated yarn's filament are improved when higher draw ratios are applied. The draw ratios of 1.20 and 1.25 cause an improvement in the filaments' breaking tenacity and breaking extension. After drawing, the elasticity modulus of the threads' filaments is lower for all draw ratios (Table II). Namely, the thread twist causes the torsion and compressive loadings of the thread-twisted filaments. This phe-

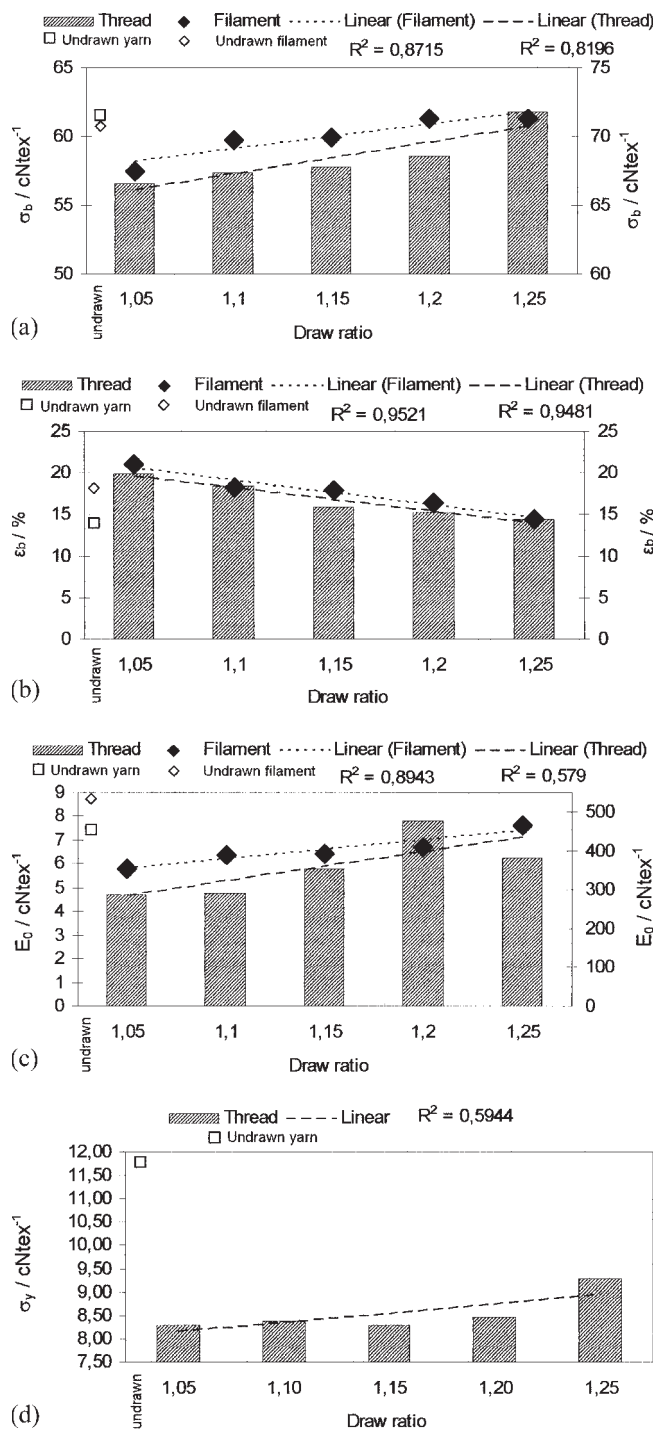


**Figure 5** Mechanical properties of the undrawn yarn, drawn threads, and their filaments: (a) breaking tenacity, (b) breaking extension, (c) elasticity modulus, (d) tension at yield point.

nomenon influences the mechanical properties, especially the elasticity modulus. Furthermore, after drawing the thread, when compared to the untreated yarn, had lower values for breaking tenacity, tension at the yield point, and elasticity modulus, and higher values for breaking extension at all draw ratios

(Table II). It is well-known that the breaking tenacity of the thread is lower in comparison to the breaking tenacity of the thread-twisted yarns/filaments, due to the twisting of the thread. When twisting, the thread achieves a spiral form. In this form, the filaments are inclined at a defined angle in regard to the thread axis, which decreases the tensile strength of the thread's filaments and increases the breaking extension.<sup>29,30</sup>

There is a relationship between the mechanical properties of the thread and the filaments forming the thread. Both are influenced by the drawing conditions and by the twist. It was found that improvement in mechanical properties causes structural modification of the filaments, and straightening of the filaments in the thread construction by drawing, which increase the breaking tenacity, elasticity modulus, and tension at the yield point and decreases the breaking extension. Drawing of the sewing thread has greater influence on the breaking extension, elasticity modulus, and thread tension at the yield point when compared to the breaking tenacity.

## CONCLUSIONS

Sewing thread drawing conditions that comprise thermal treatment and mechanical deformations cause significant changes in filament structure. We suppose that the temperature on the first cylinder, and induced strain, cause orientation of the molecular segments in the noncrystalline regions, while the conditions on the second cylinder, i.e., the temperature and thermal treatment time on the second cylinder, mainly affects the crystalline filament structure. In addition, an increase is observed in birefringence. The increased molecular orientation and crystallinity are reasons for the improvement in the mechanical properties of the sewing thread.

In our investigation, dependence among the draw ratios, structural parameters, and mechanical properties was confirmed, i.e., a higher draw ratio increases the birefringence, amorphous orientation, and degree of crystallinity, as well as breaking tenacity, elasticity modulus, tension at the yield point, and decreases the breaking extension. The mechanical properties of the threads are also influenced by loadings when twisting the thread. Therefore, an improvement in the filament's mechanical properties is achieved at higher draw ratios when compared with the untreated filaments' mechanical properties.

For the reason of  $\beta$ -relaxation transition's (glass-transition) improvement, it was established that by thread drawing improvement in the yield point can be achieved, which can assure the high quality thread needed for good resistance against dynamic and thermal load during the sewing process.

## References

1. Murayama, T. *Dynamic Mechanical Analysis of Polymeric Material*; Elsevier Scientific Publishing: Amsterdam, 1978.
2. Ward, I. M.; Hadley, D. W. *An Introduction to the Mechanical Properties of Solid Polymers*; Wiley: England, 1995.
3. Aji, A.; Cole, K. C.; Dumoulin, M. M.; Brisson, J. *Polymer* 1995, 36, 4023.
4. Aji, A.; Guèvremont, J.; Cole, K. C.; Dumoulin, M. M. *Polymer* 1996, 37, 3707.
5. Geršak, J. 1. *Dresdner Textiltagung '92*, Technische Universität Dresden, Dresden, Vorträge Teil 2 1992, 272.
6. Cullerton, D. L.; Ellison, M. S.; Aspland, J. R. *Textile Res J* 1990, 50, 594.
7. Elenga, R.; Seguela, R.; Rietsch, F. *Polymer* 1991, 32, 1975.
8. Göschel, U.; Urban, G. *Polymer* 1995, 36, 3633.
9. Gupta, V. B.; Kumar, S. *J Appl Polym Sci* 1981, 26, 1865.
10. Gupta, V. B.; Kumar, S. *J Appl Polym Sci* 1981, 26, 1877.
11. Gupta, V. B.; Kumar, S. *J Appl Polym Sci* 1981, 26, 1897.
12. Pal, S. K.; Ghandhi, R. S.; Kothari, V. K. *Chem Fibers Int* 1995, 45, 418.
13. Peterlin, A. *Textile Res J* 1972, 42, 20.
14. Samuels, R. J. *J Polym Sci Part A-2: Polym Phys* 1972, 10, 781.
15. ASTM D2102-96. *Standard Test Method for Shrinkage of Textile Fiber Bundle Test*, ASTM International, 1996.
16. Bukošek, V. *Tekstilec* (in Slovene) 1983, 26, 24.
17. Nettelstroth, K. *Melliand Textilberichte* 1972, 63, 212.
18. ISO 2062. *Textiles—Yarn from packages—Method for determination of breaking load and elongation at the breaking load of single strands—(CRL, CRE and CRT testers)*, First edition, International Organization for Standardization, 1972.
19. ISO 5079. *Textiles—Man-made fibres—Determination of breaking strength and elongation of individual fibres*, International Organization for Standardization, 1977.
20. Widmann, G.; Riesen, R. *Thermal Analysis*; Dr. Alfred Hüthling Verlag: Heidelberg, 1987.
21. Wunderlich, B. *Molecular Physics*; Academic Press: New York, 1980; Vol. 3, p 68.
22. ISO 139. *Textiles—Standard atmospheres for conditioning and testing*, First edition, International Organization for Standardization, 1973.
23. ISO 1889. *Textiles—Determination of linear density of single and plied yarns (reel method)*, International Organization for Standardization, 1987.
24. Lewin, M.; Pearce, E. M. *Handbook of Fiber Science and Technology, Volume IV: Fiber Chemistry*; Marcel Dekker: New York, 1985.
25. Kunugi, T.; Suzuki, A. *J Appl Polym Sci* 1996, 62, 713.
26. Van Den Heuvel, C. J. M.; Heuvel, H. M.; Faassen, W. A.; Veurink, J.; Lucas, L. J. *J Appl Polym Sci* 1993, 49, 25.
27. Suzuki, A.; Mochiduki, N. *J Appl Polym Sci* 2001, 82, 2775.
28. Žiberna Šujica, M.; Šfiligoj Smole, M. *J Appl Polym Sci* 2003, 89, 3383.
29. Eirich, F. R. *Rheology, Theory and Applications: The Geometry of Tensional Behaviour of Yarns*; Polytechnic Institute of Brooklyn: Brooklyn, New York, 1969.
30. Hearle, J. W. S.; Grosberg, P.; Backer, S. *Structural Mechanics of Fibers, Yarns and Fabrics, Vol. 1*; Wiley-Interscience: New York, 1969.